RESEARCH PAPER

PCCP
www.rsc.org/pccp

Hydrogen diffusion effects on the kinetics of the hydrogen electrode reaction. Part I. Theoretical aspects

María R. Gennero de Chialvo and Abel C. Chialvo*

Programa de Electroquímica Aplicada e Ingeniería Electroquímica (PRELINE), Facultad de Ingeniería Química, Universidad Nacional del Litoral, Santiago del Estero 2829, 3000 Santa Fe, Argentina. E-mail: achialvo@fiqus.unl.edu.ar

Received 23rd February 2004, Accepted 17th May 2004
First published as an Advance Article on the web 1st June 2004

The effect of the hydrogen diffusion on the hydrogen electrode reaction has been studied and rigorous kinetic expressions for the Tafel–Heyrovsky–Volmer mechanism has been derived. The analysis of the dependences of the current density (j) on overpotential (η), particularly oriented to the hydrogen oxidation reaction (hor), leads to the following main results: (i) in the Tafel–Volmer (TV) route, the current density reaches a maximum value (j_{max}) less or equal to the limiting diffusion current density (j_L); (ii) j_{max} is always equal to j_L for the Heyrovsky–Volmer (HV) route; (iii) in the simultaneous occurrence of both routes (THV), the current density always reaches the j_L value, although in the range of overpotentials of applied interest ($0 \leq \eta/V \leq 0.6$) the j_{max} value, characteristic of the TV route, can also be obtained.

The Levich–Koutecky plots have also been analysed and it has been demonstrated that the $j(\eta)$ dependence for the hor under activated control cannot always be obtained from these plots.

DOI: 10.1039/b402695k

Introduction

The kinetics of the hydrogen electrode reaction (HER) has mainly been studied far from equilibrium conditions. Thus, the reaction in the cathodic direction, the hydrogen evolution reaction (her), is perhaps the most studied in electrochemistry. On the contrary, the hydrogen oxidation reaction (hor) has not received the same attention, in spite of being the anodic reaction of the conventional H_2–O_2 fuel cells.[1–13] Kinetic studies near equilibrium are also very scarce.[14]

The diffusion of molecular hydrogen on both directions, towards and from the electrode surface, affects the HER in all cases, but it is of critical importance in the hor. Consequently, the kinetic study of this reaction needs well-defined hydrodynamic conditions for the experimental determinations, which are usually obtained with a rotating disc electrode. It has been demonstrated with this technique that the hor reaches at rather low overpotentials a constant value of the current density, which is usually assigned to the limiting diffusion current density j_L, but in this work it will be called j_{max}. Both values will be identical only if the concentration of molecular hydrogen cancels out at the electrode surface. If this condition is fulfilled, the limiting current density must be independent of any electrode pre-treatment, of any partial inhibition of the substrate surface and even of the electrode nature. Nevertheless, there are several experimental results described in the literature that show a different behaviour. Makowski *et al.*[2] obtained on a Pt electrode treated with permanganic acid a maximum current density much more higher than that of the electrode without treatment. More recently, studies carried out on Pt (hkl)[11] show clearly that the limiting current density decreases in the presence of $Bi_{(ad)}$. This result cannot be explained as an inhibition process because if, for instance, 50% of the surface sites are inhibited, the limiting diffusion current could be maintained by duplicating the current density on the active surface sites.

Other interesting results are the existence of origin intercepts different from zero in the Levich–Koutecky diagrams corresponding to the limiting currents. In numerous works, the experimental dependences $j_{max}^{-1} = f(\omega^{-1/2})$, ω being the rotation rate, were adjusted by straight lines passing through zero, but this was clearly not the best linear correlation.[1–3,6–8,15] In this sense, Yeager *et al.*[7] emphasised that the origin intercept was still quite finite within experimental error. These evidences, which are inconsistent with the assumption that the maximum current is originated in a pure diffusion control, indicate that a revision of the usual interpretation of the experimental results is necessary.

The present work deals with theoretical aspects related to the effect of the diffusion of molecular hydrogen on the HER, particularly oriented to the hor, resulting on a more rigorous formalism than that currently used.

Basic equations

The hydrogen oxidation reaction (hor):

$$H_{2(g)} \rightleftharpoons 2H^+ + 2e^- \qquad (1)$$

involves the following elementary steps:

$$H_{2(g)} + 2S \underset{v_{-T}}{\overset{v_{+T}}{\rightleftharpoons}} H_{(a)} + H_{(a)} \quad \text{Tafel} \qquad (2a)$$

$$H_{2(g)} + S \underset{v_{-H}}{\overset{v_{+H}}{\rightleftharpoons}} H^+ + H_{(a)} + e^- \quad \text{Heyrovsky} \qquad (2b)$$

$$H_{(a)} + S \underset{v_{-V}}{\overset{v_{+V}}{\rightleftharpoons}} H^+ + e^- \quad \text{Volmer} \qquad (2c)$$

where S is an adsorption site. As there are three elementary steps and only one intermediate species, the whole reaction can be verified through two independent routes,[16] which in this case are the Tafel–Volmer and Heyrovsky–Volmer routes. Taking into account that in steady state the mass balance of each participant of the elementary reactions (2a–c) must satisfy the corresponding mass balance of the whole reaction (1), the following relationships can be derived for the simultaneous occurrence of the two routes:

$$j = 2Fv = F(v_v + v_H) = 2F(v_H + v_T) = 2F(v_V - v_T) \qquad (3)$$

where $v_i = v_{+i} - v_{-i}$; i = V, H, T. v is the rate of reaction (1), v_i is the rate of the elementary step i, v_{+i} and v_{-i} being the rates of the forward and backward reaction of the step i, respectively. It should be noted that eqn. (3) is independent of the direction in which reaction (1) is verified, and therefore it is applicable to both the hor as well as the her.[17] It has been considered that only the concentration of molecular hydrogen decreases in the plane of reaction with respect to the bulk concentration. This is equivalent to considering that polarisation due to protons concentration is negligible. Therefore, the rates of the elementary steps are:

$$v_T = v_T^e\left[\left(\frac{1-\theta}{1-\theta^e}\right)^2\left(\frac{P_{H_2}^s}{P_{H_2}^e}\right) - \left(\frac{\theta}{\theta^e}\right)^2\right] \quad (4a)$$

$$v_H = v_H^e\left[\left(\frac{1-\theta}{1-\theta^e}\right)\left(\frac{P_{H_2}^s}{P_{H_2}^e}\right)e^{\alpha f\eta} - \left(\frac{\theta}{\theta^e}\right)e^{-(1-\alpha)f\eta}\right] \quad (4b)$$

$$v_V = v_V^e\left[\left(\frac{\theta}{\theta^e}\right)e^{\alpha f\eta} - \left(\frac{1-\theta}{1-\theta^e}\right)e^{-(1-\alpha)f\eta}\right] \quad (4c)$$

where η is the overpotential, θ is the surface coverage of the adsorbed hydrogen $H_{(a)}$, $P_{H_2}^s$ is the hydrogen pressure at the electrode surface, α is the symmetry factor (considered the same for the Volmer and Heyrovsky steps), $f = F/RT$ and the superscript "e" indicates equilibrium conditions. Furthermore, it has taken positive values for v and η in the anodic direction.

The rates v_i^e are given by:

$$v_T^e = k_{+T}(1-\theta^e)^2 P_{H_2}^e = k_{-T}(\theta^e)^2 \quad (5a)$$

$$v_H^e = k_{+H}(1-\theta^e)P_{H_2}^e e^{\alpha fE^e} = k_{-H}\theta^e a_{H^+}e^{-(1-\alpha)fE^e} \quad (5b)$$

$$v_V^e = k_{+V}\theta^e e^{\alpha fE^e} = k_{-V}(1-\theta^e)a_{H^+}e^{-(1-\alpha)fE^e} \quad (5c)$$

where k_{+i} and k_{-i} are the forward and backward specific rate constants of the elementary step i (i = V, H, T) respectively, a_{H^+} is the activity of protons and E^e is the equilibrium potential of the HER.

The relationship $P_{H_2}^s/P_{H_2}^e$ depends on the current density and it can only achieve a steady state if the thickness of the diffusion layer (δ) is constant, which can be experimentally obtained with a rotating disc electrode. Taking into account that the hydrogen solubility is very low in the electrolyte solution, Henry's law is applicable $\left(P_{H_2}^s = k_{H_2}c_{H_2}^s\right)$. In these conditions, the relationship is:[18]

$$\frac{P_{H_2}^s}{P_{H_2}^e} = 1 - \frac{j(\eta)}{j_L} \quad (6)$$

with j_L being the current density when $P_{H_2}^s = 0$. Consequently, incorporating eqn. (6) into eqns. (4a) and (4b) gives:

$$v_T = v_T^e\left[\left(\frac{1-\theta}{1-\theta^e}\right)^2\left(1-\frac{j}{j_L}\right) - \left(\frac{\theta}{\theta^e}\right)^2\right] \quad (7a)$$

$$v_H = v_H^e\left[\left(\frac{1-\theta}{1-\theta^e}\right)\left(1-\frac{j}{j_L}\right)e^{\alpha f\eta} - \left(\frac{\theta}{\theta^e}\right)e^{-(1-\alpha)f\eta}\right] \quad (7b)$$

The incorporation of eqns. (7a), (7b) and (4c) into eqn. (3) gives different expressions that describe the dependence of the current density on the overpotential:

$$\begin{aligned} j &= \frac{\left(\frac{\theta}{\theta^e}\right)\left[v_V^e e^{\alpha f\eta} - v_H^e e^{-(1-\alpha)f\eta}\right] + \left(\frac{1-\theta}{1-\theta^e}\right)\left[v_H^e e^{\alpha f\eta} - v_V^e e^{-(1-\alpha)f\eta}\right]}{\left[\frac{1}{F} + \left(\frac{1-\theta}{1-\theta^e}\right)\frac{v_H^e}{j_L}e^{\alpha f\eta}\right]} \\ &= \frac{v_H^e\left[\left(\frac{1-\theta}{1-\theta^e}\right)e^{\alpha f\eta} - \left(\frac{\theta}{\theta^e}\right)e^{-(1-\alpha)f\eta}\right] + v_T^e\left[\left(\frac{1-\theta}{1-\theta^e}\right)^2 - \left(\frac{\theta}{\theta^e}\right)^2\right]}{\left[\frac{1}{2F} + \left(\frac{1-\theta}{1-\theta^e}\right)\frac{v_H^e}{j_L}e^{\alpha f\eta} + \left(\frac{1-\theta}{1-\theta^e}\right)^2\frac{v_T^e}{j_L}\right]} \\ &= \frac{v_V^e\left[\left(\frac{\theta}{\theta^e}\right)e^{\alpha f\eta} - \left(\frac{1-\theta}{1-\theta^e}\right)e^{-(1-\alpha)f\eta}\right] - v_T^e\left[\left(\frac{1-\theta}{1-\theta^e}\right)^2 - \left(\frac{\theta}{\theta^e}\right)^2\right]}{\left[\frac{1}{2F} - \left(\frac{1-\theta}{1-\theta^e}\right)^2\frac{v_T^e}{j_L}\right]} \end{aligned} \quad (8)$$

In order to establish the dependence $j = j(\eta, j_L, \theta^e)$ it is necessary to know the corresponding dependence $\theta = \theta(\eta, j_L, \theta^e)$, which can be obtained, for instance, rearranging the equality between the second and third members of eqn. (8):

$$\begin{aligned} &\left[\left(\frac{1-\theta}{1-\theta^e}\right)e^{-(1-\alpha)f\eta} - \left(\frac{\theta}{\theta^e}\right)e^{\alpha f\eta}\right] \\ &\left\{v_V^e + \left(\frac{1-\theta}{1-\theta^e}\right)\frac{2F}{j_L}\left[\left(\frac{1-\theta}{1-\theta^e}\right)v_T^e v_V^e\right.\right. \\ &\left.\left.+\left(\frac{\theta}{\theta^e}\right)v_T^e v_H^e + v_V^e v_H^e e^{\alpha f\eta}\right]\right\} \\ &+ 2v_T^e\left[\left(\frac{1-\theta}{1-\theta^e}\right)^2 - \left(\frac{\theta}{\theta^e}\right)^2\right] \\ &+ v_H^e\left[\left(\frac{1-\theta}{1-\theta^e}\right)e^{\alpha f\eta} - \left(\frac{\theta}{\theta^e}\right)e^{-(1-\alpha)f\eta}\right] = 0 \end{aligned} \quad (9)$$

The simulation of the dependences of the current density on the overpotential, for given values of the parameters θ^e, J_L and v_i^e, can be performed with eqns. (8) and (9).

Analysis of the $j(\eta)$ dependences

The Tafel–Heyrovsky–Volmer mechanism used to describe the hor has two independent routes, Tafel–Volmer and Heyrovsky–Volmer, respectively. In order to evaluate the contribution of these routes to the kinetic mechanism, they will be analysed separately and then the simultaneous occurrence of the three steps will be studied. The simulations were carried out at 25 °C and the limiting current density was varied in the experimental range $10^{-3} \leq j_L/\mathrm{A\ cm^{-2}} \leq 10^{-2}$. The corresponding values of the parameters v_i^e (i = T, H, V) are indicated for each case in units of mol $\mathrm{cm^{-2}\ s^{-1}}$.

Tafel–Volmer route

The following expressions are obtained by making $v_H^e = 0$ in eqns. (8) and (9):

$$\begin{aligned} j &= Fv_V^e\left[\left(\frac{\theta}{\theta^e}\right)e^{\alpha f\eta} - \left(\frac{1-\theta}{1-\theta^e}\right)e^{-(1-\alpha)f\eta}\right] \\ &= \frac{2Fv_T^e\left[\left(\frac{1-\theta}{1-\theta^e}\right)^2 - \left(\frac{\theta}{\theta^e}\right)^2\right]}{\left[1 + \left(\frac{1-\theta}{1-\theta^e}\right)^2\frac{2Fv_T^e}{j_L}\right]} \end{aligned} \quad (10)$$

$$\begin{aligned} &v_V^e\left[\left(\frac{1-\theta}{1-\theta^e}\right)e^{-(1-\alpha)f\eta} - \left(\frac{\theta}{\theta^e}\right)e^{\alpha f\eta}\right]\left[1 + \frac{2Fv_T^e}{j_L}\left(\frac{1-\theta}{1-\theta^e}\right)^2\right] \\ &+2v_T^e\left[\left(\frac{1-\theta}{1-\theta^e}\right)^2 - \left(\frac{\theta}{\theta^e}\right)^2\right] = 0 \end{aligned} \quad (11)$$

In order to evaluate the descriptive capability of eqns. (10) and (11), the dependences $j = j(\eta, j_L)$, and $\theta = \theta(\eta, j_L)$ were

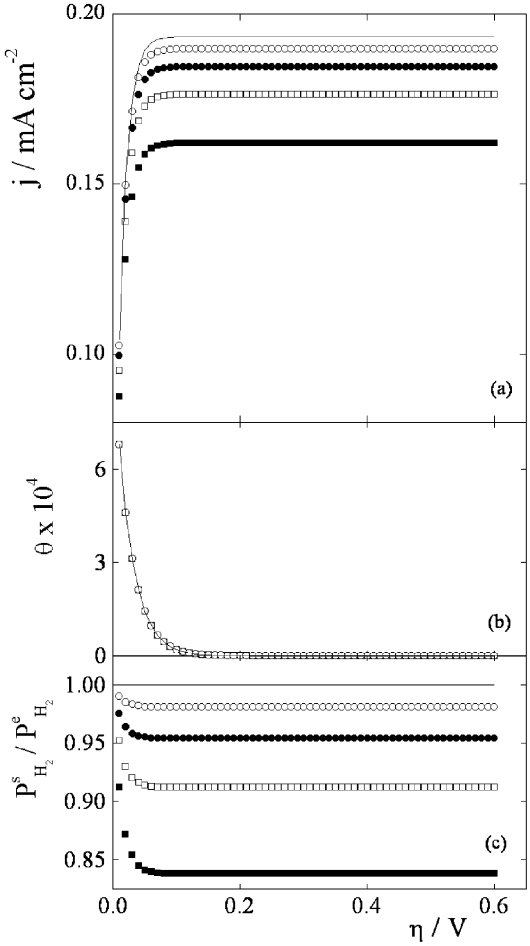

Fig. 1 (a) $j(\eta)$, (b) $\theta(\eta)$ and (c) $P^{s}_{H_2}/P^{e}_{H_2}(\eta)$ dependences of the hor for the TV route. $\theta^{e} = 10^{-3}$, $v_T{}^{e} = 10^{-9}$, $v_V{}^{e} = 10^{-5}$. j_L: (■) 1, (□) 2, (●) 4, (○) 10, (—) ∞ mA cm^{-2}.

simulated. The parameters were adjusted to $\theta^{e} = 10^{-3}$, $v_T{}^{e} = 10^{-9}$, $v_v{}^{e} = 10^{-5}$ and $10^{-3} \leq j_L/\mathrm{A\ cm^{-2}} \leq 10^{-2}$. The simulation curves corresponding to $j(\eta, j_L)$, $\theta(\eta, j_L)$, and $P^{s}_{H_2}/P^{e}_{H_2} = f(\eta, j_L)$ are illustrated in Fig. 1a–c, respectively. The results obtained can be summarised as:

(i) For the case $j_L \rightarrow \infty$ (activated control), a maximum kinetic current density is defined ($j_{max}{}^{kin}$)[19] when $\theta(\eta) \rightarrow 0$, which according to eqn. (10) is given by:

$$j^{kin}_{max} = \frac{2Fv^{e}_{T}}{(1-\theta^{e})^{2}} \qquad (12)$$

Besides, as eqn. (12) corresponds to the activated control, $P^{s}_{H_2}/P^{e}_{H_2} = 1$.

(ii) When $j_L < \infty$, the values of the constant current densities are less than j_L and therefore, from eqn. (6), $0 < P^{s}_{H_2}/P^{e}_{H_2} \leq 1$. This behaviour is due to the fact that the surface coverage cancels out while the surface hydrogen concentration is still finite. Therefore, applying the condition $\theta(\eta) = 0$ in eqn. (10), it is demonstrated that a maximum current density can be achieved before the condition for the diffusion current density is fulfilled:

$$j_{max} = \frac{2Fv^{e}_{T}}{(1-\theta^{e})^{2} + \frac{2Fv^{e}_{T}}{j_L}} \qquad (13)$$

This result can be more clearly appreciated through the analysis of the Levich–Koutecky dependence:

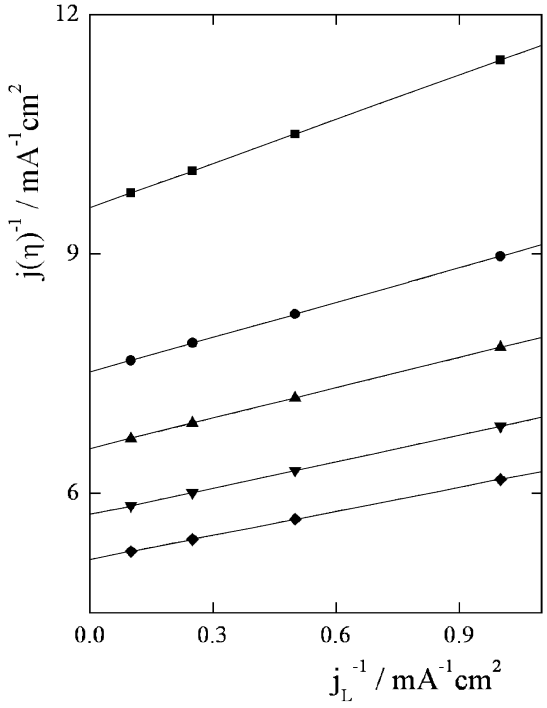

Fig. 2 $j^{-1} = f(j_L{}^{-1})$ dependences for the simulations shown in Fig. 1. η: (■) 0.01, (●) 0.015, (▲) 0.02, (▼) 0.03, (◆) 0.2 (≡ ∞) V.

$$\frac{1}{j_{max}} = \frac{(1-\theta^{e})^{2}}{2Fv^{e}_{T}} + \frac{1}{j_L} = \frac{1}{j^{kin}_{max}} + \frac{1}{j_L} \qquad (14)$$

It can be observed from eqn. (14) that the relationship is linear, but the origin intercept is different from zero, which does not agree with the commonly expected result. The dependence $j_{max}{}^{-1} = f(j_L{}^{-1})$ obtained from Fig. 1a is shown in Fig. 2 (◆ points). A linear regression of these points gave a slope equal to 1.0 and an origin intercept equal to 5.1718 mA^{-1} cm^{2}, which is coincident with the theoretical value obtained from eqn. (14). Besides, if $(1-\theta^{e})^{2} \ll 2Fv_T{}^{e}/j_L$, then $j_{max} \rightarrow j_L$. Consequently, it should be interesting to analyse a case in which this condition is fulfilled. Fig. 3 illustrates the results obtained for $\theta^{e} = 10^{-3}$, $v_T{}^{e} = 10^{-5}$ and $v_V{}^{e} = 10^{-7}$ in the same range of j_L values. In this case, $2Fv_T{}^{e}/j_L \cong 10^{3} \gg (1-\theta^{e})^{2} \cong 1$. It can be observed that the maximum current densities are practically identical to the limiting current densities.

The corresponding relationships $[j(\eta, jL)]^{-1} = f(j_L{}^{-1})$ at constant overpotential for the two cases under study are shown in Figs. 2 and 4, respectively. It should be noted that these dependences are linear in the range of j_L analysed, for any overpotential value.

Heyrovsky–Volmer route

Introducing the condition $v_T{}^{e} = 0$ into eqns. (8) and (9), the following expressions of the dependences $j(\eta)$ and $\theta(\eta)$ for the Heyrovsky–Volmer route are obtained:

$$j = \frac{2Fv^{e}_{H}\left[\left(\frac{1-\theta}{1-\theta^{e}}\right)e^{\alpha f\eta} - \left(\frac{\theta}{\theta^{e}}\right)e^{-(1-\alpha)f\eta}\right]}{\left[1 + \left(\frac{1-\theta}{1-\theta^{e}}\right)\frac{Fv^{e}_{H}}{j_L}e^{\alpha f\eta}\right]} \qquad (15)$$

$$v^{e}_{V}\left[\left(\frac{1-\theta}{1-\theta^{e}}\right)e^{-(1-\alpha)f\eta} - \left(\frac{\theta}{\theta^{e}}\right)e^{\alpha f\eta}\right]\left[1 + v^{e}_{H}e^{\alpha f\eta}\right] + v^{e}_{H}\left[\left(\frac{1-\theta}{1-\theta^{e}}\right)e^{\alpha f\eta} - \left(\frac{\theta}{\theta^{e}}\right)e^{-(1-\alpha)f\eta}\right] = 0 \qquad (16)$$

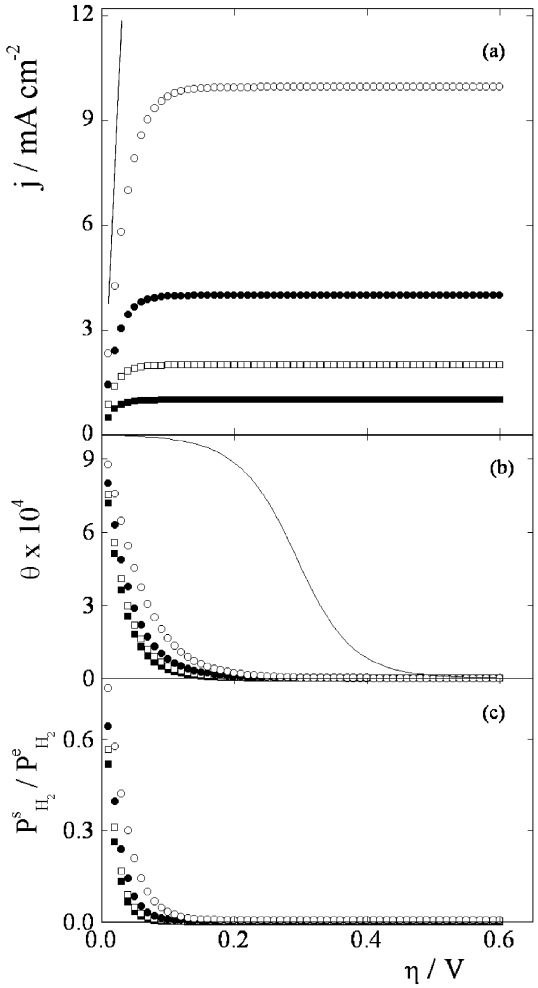

Fig. 3 (a) $j(\eta)$, (b) $\theta(\eta)$ and (c) $P^{s}_{H_2}/P^{e}_{H_2}(\eta)$ dependences of the hor for the TV route. $\theta^{e} = 10^{-3}$, $v_T{}^{e} = 10^{-5}$, $v_V{}^{e} = 10^{-7}$. j_L: (■) 1, (□) 2, (●) 4, (○) 10, (—) ∞ mA cm^{-2}.

The simulation curves corresponding to $j(\eta, j_L)$, $\theta(\eta, j_L)$ and $P^{s}_{H_2}/P^{e}_{H_2} = f(\eta, j_L)$ are illustrated in Fig. 5a, b and c, respectively for the values $\theta^{e} = 0.1$, $v_H{}^{e} = 10^{-10}$, $v_V{}^{e} = 10^{-5}$ and

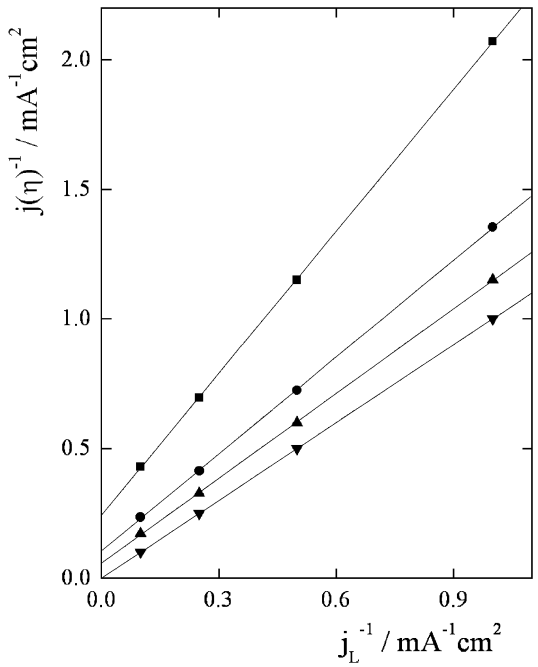

Fig. 4 $j^{-1} = f(j_L{}^{-1})$ dependences for the simulations shown in Fig. 3. η: (■) 0.01, (●) 0.02, (▲) 0.03, (▼) 0.2 (≡ ∞) V.

$10^{-3} \leq j_L/\text{A cm}^{-2} \leq 10^{-2}$. The case in which $v_V{}^{e} < v_H{}^{e}$ is shown in Fig. 6 with the parameters $\theta^{e} = 0.1$, $v_H{}^{e} = 10^{-5}$ and $v_V{}^{e} = 10^{-8}$. It can be observed that in both cases, the maximum current density is always equal to the limiting current density, as it can be derived from eqn. (15). This is the result of the simultaneous tendency to zero of both the surface coverage and the surface concentration of molecular hydrogen, as it can be verified by substitution of eqn. (15) into eqn. (6). These results are clearly observed in parts b and c of Figs. 5 and 6. Therefore, for the Heyrovsky–Volmer route, the relationship $j_{max}{}^{-1} = f(j_L{}^{-1})$ will always be a straight line without a finite origin intercept, which is a different behaviour with respect to the Tafel–Volmer route.

The corresponding relationships $[j(\eta, j_L)]^{-1} = f(j_L{}^{-1})$ at different overpotentials for the two cases analysed here are shown in Figs. 7 and 8, respectively. It should be noted that, as in the Tafel–Volmer route, these dependences are linear in the range of j_L analysed, for all overpotentials.

Simultaneous occurrence of Tafel, Heyrovsky and Volmer steps

It has been demonstrated in the previous items that the kinetic behaviour of the Tafel–Volmer (TV) and Heyrovsky–Volmer (HV) routes are markedly different. While in the first case it is possible that $j_{max} < j_L$, in the second one the condition $j_{max} = j_L$ is always verified. The simultaneous occurrence of these two routes will always be conditioned, at sufficiently high overpotential values, by the Heyrovsky elementary step. However, the range of η values of experimental interest for the hor is

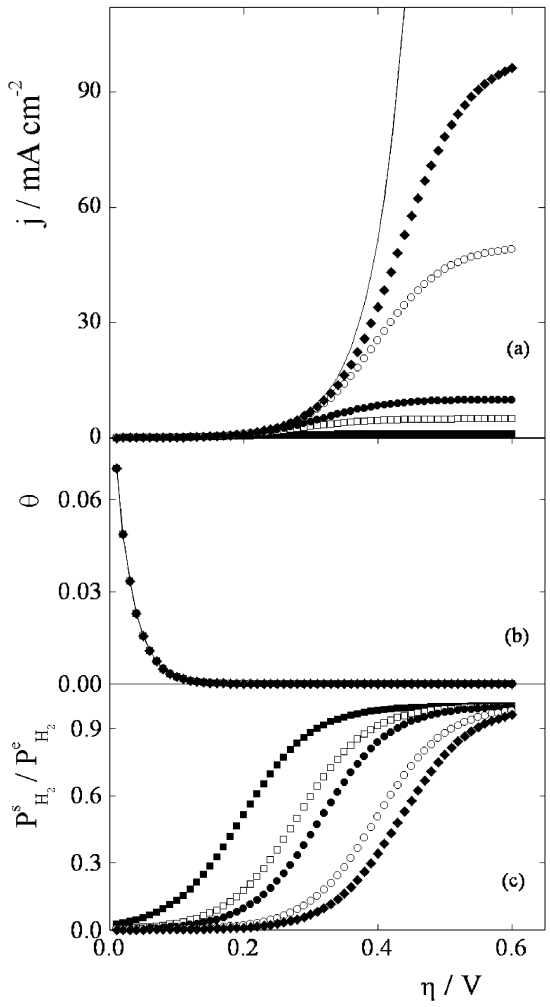

Fig. 5 (a) $j(\eta)$, (b) $\theta(\eta)$ and (c) $P^{s}_{H_2}/P^{e}_{H_2}(\eta)$ dependences of the hor for the HV route. $\theta^{e} = 0.1$, $v_H{}^{e} = 10^{-10}$, $v_V{}^{e} = 10^{-5}$. j_L: (■) 1, (□) 2, (●) 5, (○) 8, (◆) 10, (—) ∞ mA cm^{-2}.

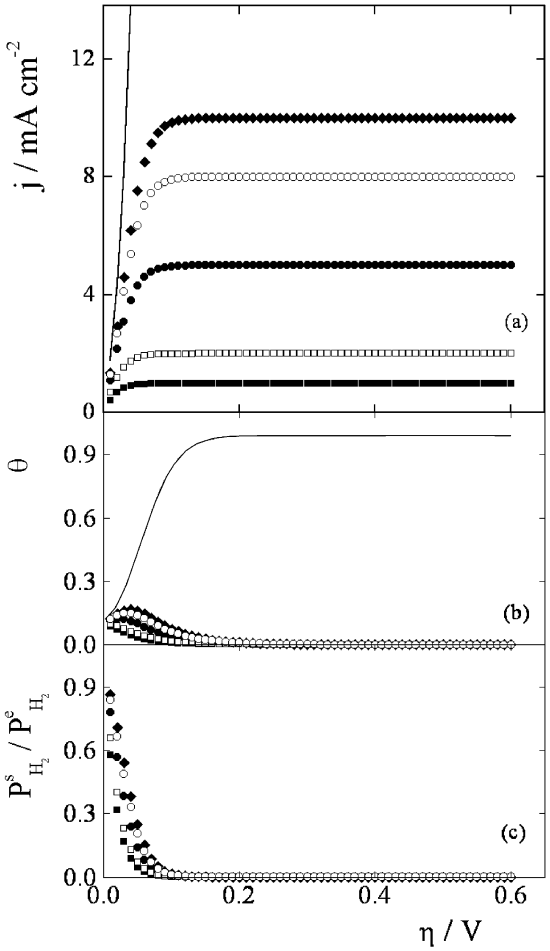

Fig. 6 (a) $j(\eta)$, (b) $\theta(\eta)$ and (c) $P^{s}_{H_2}/P^{e}_{H_2}(\eta)$ dependences of the hor for the HV route. $\theta^{e} = 0.1$, $v_H{}^{e} = 10^{-5}$, $v_V{}^{e} = 10^{-8}$. j_L: (■) 1, (□) 2, (●) 5, (○) 8, (◆) 10, (—) ∞ mA cm^{-2}.

comprised between $0.0 < \eta/V \leq 0.6$ V. In this domain, the kinetic behaviour can change from TV to HV depending on the values of the parameters v_i^{e} (i = T, H, V). Consequently, the

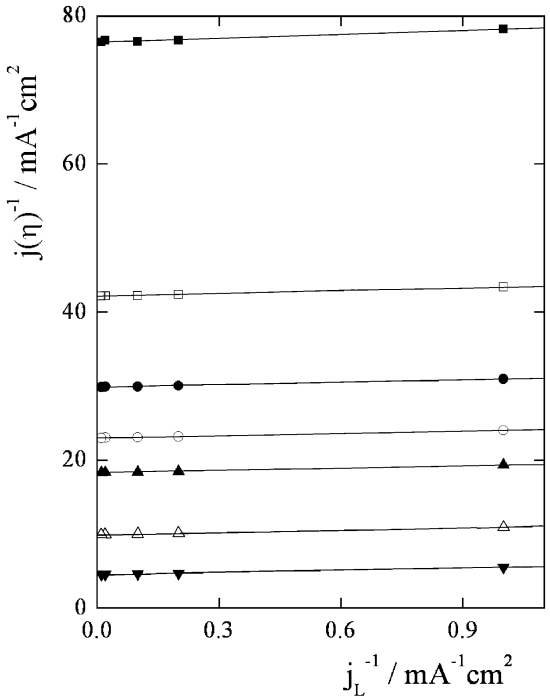

Fig. 7 $j^{-1} = f(j_L{}^{-1})$ dependences for the simulations shown in Fig. 5. η: (■) 0.01, (□) 0.02, (●) 0.03, (○) 0.04, (▲) 0.05, (△) 0.08, (▼) 0.12 V.

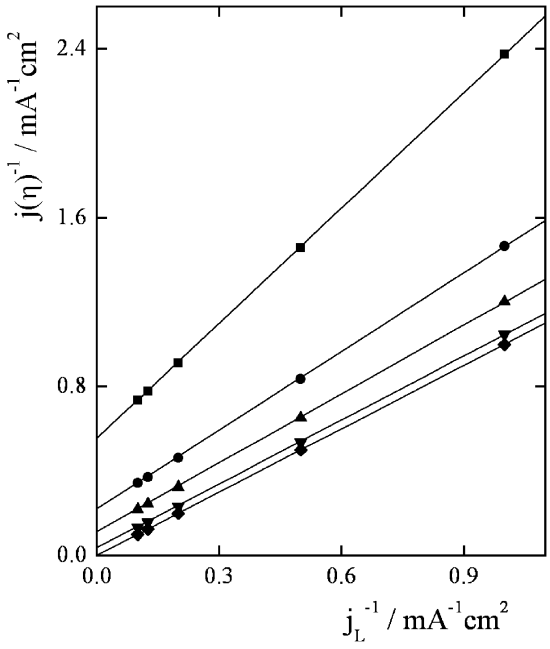

Fig. 8 $j^{-1} = f(j_L{}^{-1})$ dependences for the simulations shown in Fig. 6. η: (■) 0.01, (●) 0.02, (▲) 0.03, (▼) 0.05, (◆) 0.2 (≡ ∞) V.

descriptive capability of the simultaneous occurrence of the three elementary steps was also analysed through the use of eqns. (8) and (9).

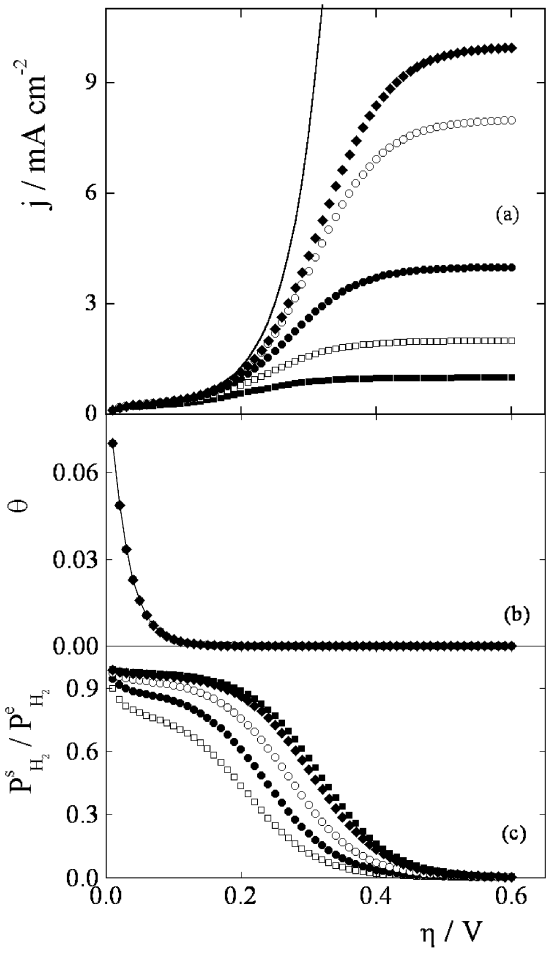

Fig. 9 (a) $j(\eta)$, (b) $\theta(\eta)$ and (c) $P^{s}_{H_2}/P^{e}_{H_2}(\eta)$ dependences of the hor for the THV route. $\theta^{e} = 0.1$, $v_T{}^{e} = 10^{-9}$, $v_H{}^{e} = 10^{-10}$, $v_V{}^{e} = 10^{-5}$. j_L: (■) 1, (□) 2, (●) 4, (○) 8, (◆) 10, (—) ∞ mA cm^{-2}.

Fig. 9 shows the simulations corresponding to the following parameters: $10^{-3} \leq j_L/\text{A cm}^{-2} \leq 10^{-2}$, $\theta^e = 0.1$, $v_T^e = 10^{-9}$, $v_H^e = 10^{-10}$ and $v_V^e = 10^{-5}$. It can be appreciated that up to $\eta \leq 0.150$ V the current densities are practically independent of j_L, defined in the range $0.03 \leq \eta/\text{V} \leq 0.13$ V an apparent plateau at $j(\eta) \cong 0.2 - 0.3$ mA cm^{-2}, together with a similar variation of the surface hydrogen concentration (Fig. 9c). This behaviour is basically determined by the Tafel–Volmer route. In this sense, it should be useful to compare the current density of this plateau with the value $j_{max} \cong 0.23$ mA cm^{-2} corresponding to the same kinetic parameters of the TV route (eqn. 12). The increase in η values produces a strong effect of j_L on $j(\eta)$ and a clear prevalence of the Heyrovsky–Volmer route, the values being $j_{max} = j_L$ reached at $\eta > 0.6$ V, as it can be demonstrated from the analysis of eqn. (8).

Furthermore, Fig. 10 shows the simulations corresponding to following parameters: $\theta^e = 0.1$, $v_T^e = 10^{-5}$, $v_H^e = 10^{-10}$ and $v_V^e = 10^{-9}$. It can be observed that in this case, the limiting diffusion current densities are clearly reached. Besides the dependences of both, surface coverage (Fig. 10b) and superficial hydrogen concentration (Fig. 10c), respectively, are clear functions of j_L.

The $[j(\eta, j_L)]^{-1} = f(j_L^{-1})$ dependences at constant overpotential for these two cases are shown in Figs. 11 and 12, respectively. It should be noticed that, as in TV and HV routes, these dependences are linear in the range of j_L analysed, for any overpotential value.

Finally, taking into account that the HER on platinum is mainly verified through the Tafel–Volmer route with a little

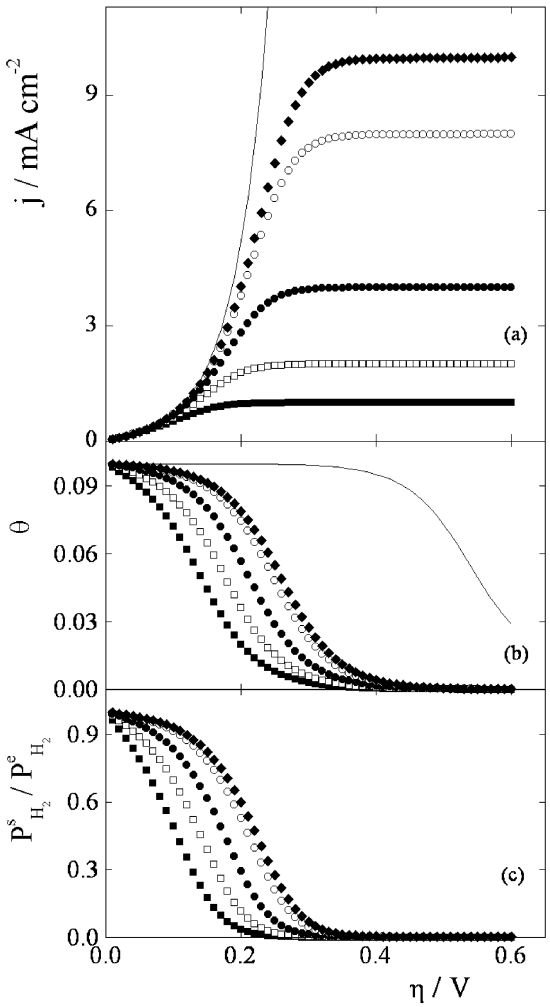

Fig. 10 (a) $j(\eta)$, (b) $\theta(\eta)$ and (c) $P^s_{H_2}/P^e_{H_2}(\eta)$ dependences of the hor for the THV route. $\theta^e = 0.1$, $v_T^e = 10^{-5}$, $v_H^e = 10^{-10}$, $v_V^e = 10^{-9}$. j_L: (■) 1, (□) 2, (●) 4, (○) 8, (◆) 10, (—) ∞ mA cm^{-2}.

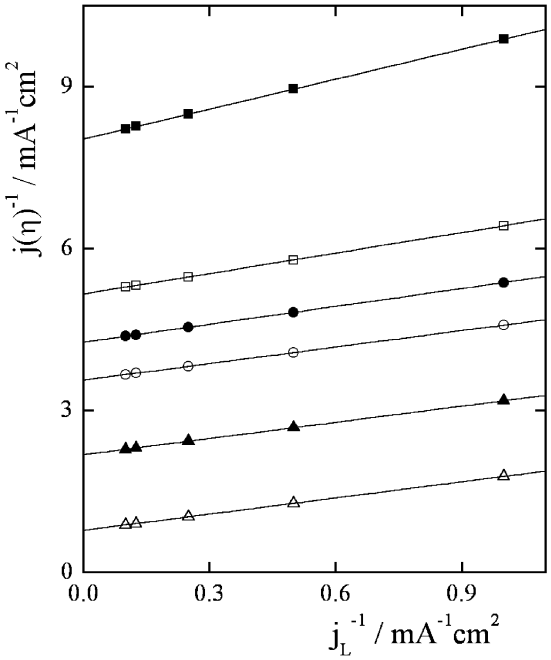

Fig. 11 $j^{-1} = f(j_L^{-1})$ dependences for the simulations shown in Fig. 9. η: (■) 0.01, (□) 0.02, (●) 0.03, (○) 0.05, (▲) 0.12, (△) 0.2 V.

contribution of the Heyrovsky–Volmer route,[14] the effect of v_H^e on the TV route is analysed. Figs. 13a–c show the dependences $j(\eta)$, $\theta(\eta)$ and $P^s_{H_2}/P^e_{H_2} = f(\eta)$ for the parameters: $\theta^e = 0.1$, $v_T^e = 10^{-8}$, and $v_V^e = 10^{-5}$, $j_L = 3$ mA cm^{-2} and $10^{-15} \leq v_H^e \leq 10^{-10}$. In the range of overpotentials analysed, $j(\eta)$ shows clearly a behaviour similar to that corresponding to the TV route for $v_H^e \leq 10^{-14}$, with a maximum current density equal to 1.3278 mA cm^{-2}, in agreement with the value obtained from eqn. (13). Nevertheless, it should be noted that if the η values continue to increase, the value $j_{max} = j_L$ must be reached, as can be appreciated for $v_H^e > 10^{-14}$ in Fig. 13a. Consequently, when $v_H^e < 10^{-14}$, the dependence $j(\eta)$ can display in the range $0 \leq \eta/\text{V} \leq 0.6$ a maximum current density, which has not originated in a diffusion process.

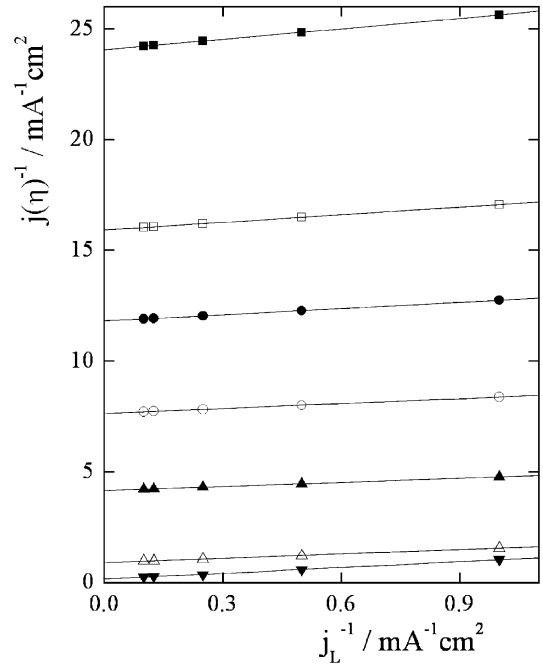

Fig. 12 $j^{-1} = f(j_L^{-1})$ dependences for the simulations shown in Fig. 10. η: (■) 0.01, (□) 0.015, (●) 0.02, (○) 0.03, (▲) 0.05, (△) 0.12, (▼) 0.2 V.

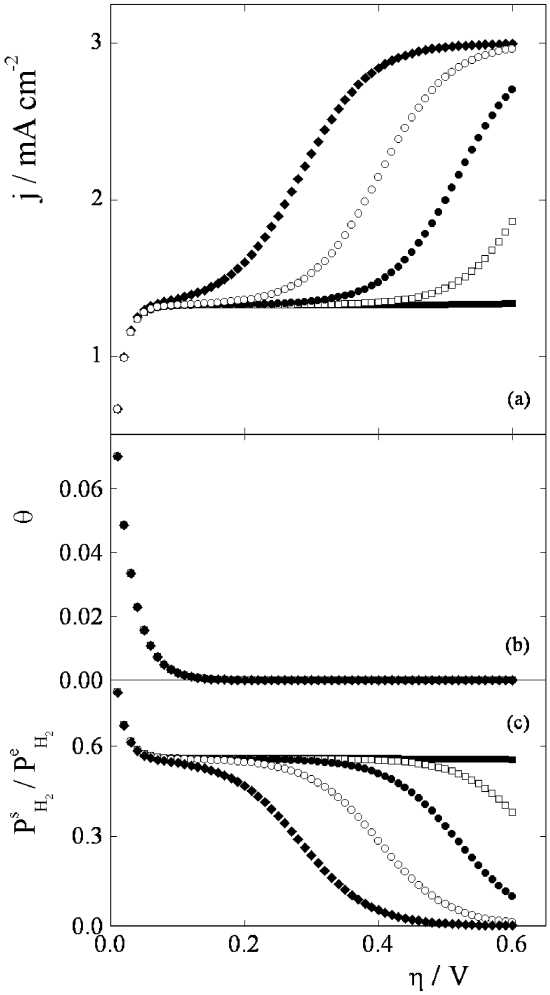

Fig. 13 (a) $j(\eta)$, (b) $\theta(\eta)$ and (c) $P^{s}_{H_2}/P^{e}_{H_2}(\eta)$ dependences of the hor for the THV route. $\theta^{e} = 0.1$, $v_T^{e} = 10^{-8}$, $v_V^{e} = 10^{-5}$, $j_L = 3$ mA cm^{-2}. v_H^{e}: (■) 10^{-15}, (□) 10^{-13}, (●) 10^{-12}, (○) 10^{-11}, (◆) 10^{-10}.

Levich–Koutecky plots

The rotating disc electrode is usually employed to carry out the experimental kinetic study of a non-catalytic electrochemical reaction under mixed control.[20] The corresponding kinetic parameters are mainly obtained from the linear extrapolation of the dependence of the inverse of current density $[j(\eta, \omega)]^{-1}$ with the inverse of the square root of the rotation rate ($\omega^{-1/2}$) at a given overpotential. Therefore, it should be of interest to analyse the applicability of the Levich–Koutecky plots for the evaluation of experimental results. Bearing in mind that j_L is proportional to $\omega^{1/2}$, eqn. (8) can be rewritten in the form, for a given overpotential η_i:

$$\frac{1}{j(\eta_i, j_L)} = a(\eta_i, j_L) + b(\eta_i, j_L)\frac{1}{j_L} \qquad (17)$$

where

$$a(\eta_i, j_L) = \left\{ 2Fv_H^{e}\left[\left(\frac{1-\theta}{1-\theta^{e}}\right)e^{\alpha f\eta_i} - \left(\frac{\theta}{\theta^{e}}\right)e^{-(1-\alpha)f\eta_i}\right] + 2Fv_T^{e}\left[\left(\frac{1-\theta}{1-\theta^{e}}\right)^{2} - \left(\frac{\theta}{\theta^{e}}\right)^{2}\right]\right\}^{-1} \qquad (18)$$

$$b(\eta_i, j_L) = \frac{\left(\frac{1-\theta}{1-\theta^{e}}\right)v_H^{e}e^{\alpha f\eta_i} + \left(\frac{1-\theta}{1-\theta^{e}}\right)^{2}v_T^{e}}{v_H^{e}\left[\left(\frac{1-\theta}{1-\theta^{e}}\right)e^{\alpha f\eta_i} - \left(\frac{\theta}{\theta^{e}}\right)e^{-(1-\alpha)f\eta_i}\right] + v_T^{e}\left[\left(\frac{1-\theta}{1-\theta^{e}}\right)^{2} - \left(\frac{\theta}{\theta^{e}}\right)^{2}\right]} \qquad (19)$$

Taking into account that eqn. (9) gives an implicit dependence $\theta = \theta(\eta, j_L)$, it would be possible to obtain a linear dependence of eqn. (17) at a given overpotential η_i, as it is established by the Levich–Koutecky expression, only for a particular domain of the kinetic parameters v_T^{e}, v_H^{e} and v_V^{e} for which $\theta = \theta(\eta)$. This condition is fulfilled when in the whole interval of j_L values (included $j_L \to \infty$) it is verified that:

$$v_V^{e} \gg \left(\frac{1-\theta}{1-\theta^{e}}\right)\frac{2F}{j_L}\left[\left(\frac{1-\theta}{1-\theta^{e}}\right)v_T^{e}v_V^{e} + \left(\frac{\theta}{\theta^{e}}\right)v_T^{e}v_H^{e} + v_V^{e}v_H^{e}e^{\alpha f\eta}\right] \qquad (20)$$

It should be noted that only when this condition is accomplished, the origin intercept $a(\eta_i, j_L)$ can be identified as the inverse of the current density corresponding to $j_L \to \infty$, that is the hor operating free of any limitation due to mass transfer. Therefore, only in this case, the usual extrapolation of the Levich-Koutecky plots is valid for the evaluation of the experimental dependence $j(\eta)$ corresponding to the hor under activated control. This can be easily appreciated for the cases corresponding to Figs. 1, 5 and 9 previously analysed. The dependences $\theta(\eta, j_L)$ shown in these figures are invariant with j_L in the range $10^{-3} \leq j_L/\text{mA cm}^{-2} < \infty$. Consequently, straight lines in the Levich–Koutecky diagram are expected, with origin intercepts equal to the inverse of the current densities corres ponding to the dependence $j(\eta)$ under activated control. The corresponding Levich–Koutecky plots are illustrated in Figs. 2, 7 and 11, respectively. The current densities obtained from the

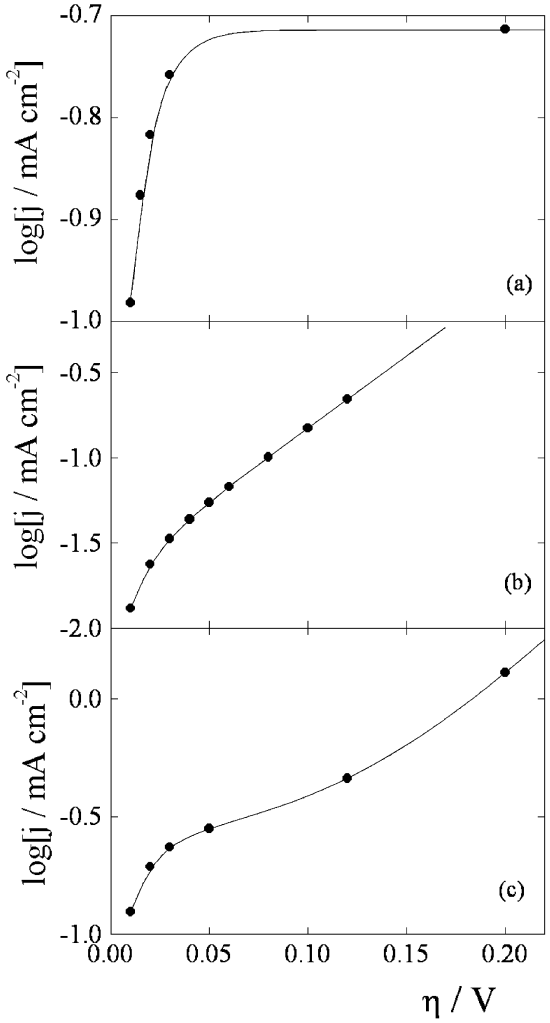

Fig. 14 log $j(\eta)$ dependences of the hor for (a) TV route (parameters of Fig. 1), (b) HV route (parameters of Fig. 5), (c) THV route (parameters of Fig. 9). (—) Activated control, (■) values obtained from extrapolations of the corresponding $j^{-1} = f(j_L^{-1})$ plots.

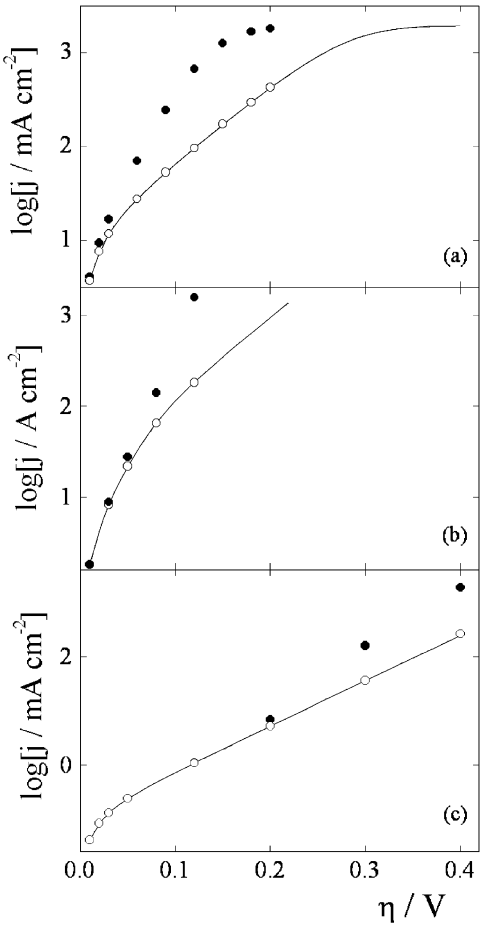

Fig. 15 log $j(\eta)$, dependences of the hor for (a) TV route (parameters of Fig. 3), (b) HV route (parameters of Fig. 6), (c) THV route (parameters of Fig. 10). (—) Activated control, (●) values obtained from extrapolations of the corresponding $j^{-1} = f(j_L{}^{-1})$ plots ($10^{-3} \leq j_L$/A cm$^{-2} \leq 10^{-2}$), (○) values obtained from extrapolations of the corresponding $j^{-1} = f(j_L{}^{-1})$ plots ($j_L > 0.1$ A cm^{-2}).

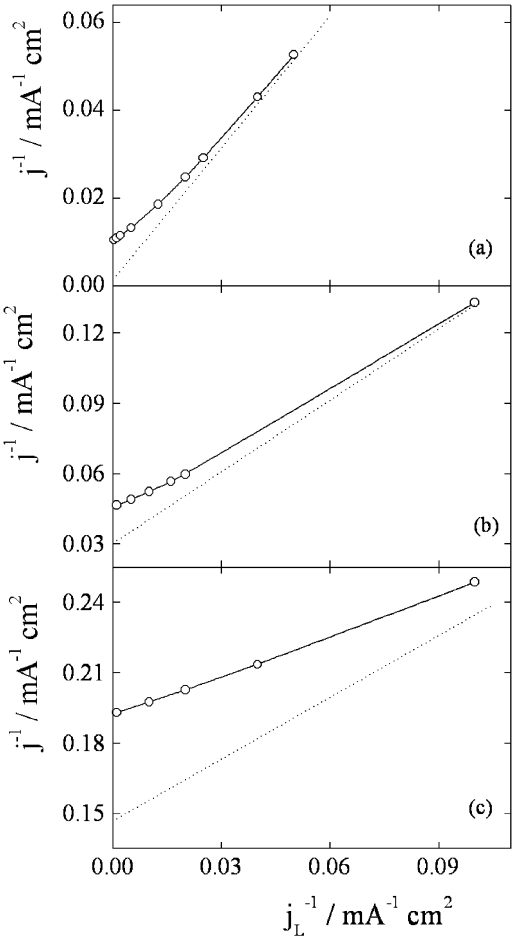

Fig. 16 $j^{-1} = f(j_L{}^{-1})$ dependences for (a) TV route (parameters of Fig. 3, $\eta = 0.12$ V), (b) HV route (parameters of Fig. 6, $\eta = 0.05$ V), (c) THV route (parameters of Fig. 10, $\eta = 0.2$ V). (○) $j_L > 0.1$ A cm^{-2}, (· · · · ·) linear extrapolation obtained from $10^{-3} \leq j_L$/A cm$^{-2} \leq 10^{-2}$.

extrapolation of all these straight lines are compared in Fig. 14a–c with the corresponding dependence $j(\eta)$ evaluated under activated control (continuous lines). The coincidence between the real $j(\eta)$ values and those obtained in the extrapolation of the Levich-Koutecky plots, can be observed.

The situation is quite different for the cases shown in Figs. 3, 6 and 10, where in the corresponding parts b it can be clearly observed that the surface coverage at constant overpotential is a function of j_L. Figs. 4, 8 and 12 illustrate the dependences $[j(\eta, j_L)]^{-1} = f(j_L{}^{-1})$ obtained from the simulations depicted in parts a of Figs. 3, 6 and 10, respectively. An apparent linear variation can be appreciated in the range of j_L values studied ($10^{-3} \leq j_L$/A cm$^{-2} \leq 10^{-2}$). Nevertheless, the comparison between the current density values obtained from the extrapolation (Fig. 15a–c, filled circles) and those obtained through the simulation under activated control (Fig. 15a–c, continuous lines) indicates that the extrapolations of the Levich–Koutecky plots are completely wrong.

Furthermore, the following limiting condition must be fulfilled:

$$\lim_{j_L \to \infty} j(\eta_i, j_L) = j(\eta_i) \qquad (21)$$

Therefore, in order to satisfy this condition, j_L values should be increased. The dependences $[j(\eta, j_L)]^{-1} = f(j_L{}^{-1})$ obtained for $j_L > 0.1$ A cm^{-2} are shown in Fig. 16a–c for the cases corresponding to the simulations illustrated in parts a of Figs. 3, 6 and 10. Nevertheless, it should be borne in mind that these j_L values cannot be reached with a rotating disc electrode. The non linear behaviour and the difference between the origin intercepts of the extrapolations of these curves and those corresponding to the straight lines obtained in the region of experimental j_L values (dot lines), can be clearly appreciated. The open circles in Fig. 15a–c correspond to the current density values obtained from the nonlinear extrapolations in the range of high j_L values and the complete agreement with the simulation under activated control can be observed (Fig. 15a–c, continuous lines).

It can be concluded that although in the domain of experimentally measurable j_L values for the hor in aqueous solutions ($10^{-3} \leq j_L$/A cm$^{-2} \leq 10^{-2}$) the Levich–Koutecky diagrams can be linear, as in all the simulations carried out in this work, this result does not ensure the agreement between the inverse of the origin intercepts and the current densities under activated control at a given overpotential. Consequently, it should be necessary to continue this study in order to develop a method for the evaluation of the kinetic parameters from experimental determinations. This topic will be discussed in the next parts of the present work.

Acknowledgements

The financial support of Consejo Nacional de Investigaciones Científicas y Técnicas (CONICET), Agencia Nacional de Promoción Científica y Tecnológica (ANPCYT) and Universidad Nacional del Litoral is gratefully acknowledged.

References

1 E. A. Aikozyan and A. J. Federova, *Proc. Acad. Sci., USSR*, 1952, **86**, 1137–1140.
2 M. P. Makowski, E. Hertz and E. Yeager, *J. Electrochem. Soc.*, 1966, **113**, 204–206.
3 V. V. Sobol, A. A. Dmitrieva and A. N. Frumkin, *Sov. Electrochem.*, 1967, **3**, 928–932.
4 S. Schuldiner, *J. Electrochem. Soc.*, 1968, **115**, 362–365.
5 J. A. Harrison and Z. A. Khan, *J. Electroanal. Chem.*, 1971, **30**, 327–330.
6 V. S. Bagotzky and N. V. Osetrova, *J. Electroanal. Chem.*, 1973, **43**, 233–249.
7 F. Ludwig, R. K. Sen and E. Yeager, *Sov. Electrochem.*, 1977, **13**, 717–723.
8 G. Bronoel and M. Haim, *J. Chim. Phys.*, 1978, **79**, 952–960.
9 N. M. Markovic, S. T. Sarraf, H. A. Gasteiger and P. N. Ross Jr., *J. Chem. Soc. Faraday Trans.*, 1996, **92**, 3719–3725.
10 R. M. Q. Mello and E. A. Ticianelli, *Electrochim. Acta*, 1997, **42**, 1031–1039.
11 T. J. Schmidt, B. N. Grgur, R. J. Behm, N. M. Markovic and P. N. Ross Jr., *Phys. Chem. Chem. Phys.*, 2000, **2**, 4379–4386.
12 V. Stamenkovic, N. M. Markovic and P. N. Ross, Jr., *J. Electroanal. Chem.*, 2001, **500**, 44–51.
13 H. Inone, J. X. Wang, K. Sasaki and R. R. Adzic, *J. Electroanal. Chem.*, 2003, **554–555**, 77–85.
14 J. L. Fernández, M. R. Gennero de Chialvo and A. C. Chialvo, *Phys. Chem. Chem. Phys.*, 2003, **5**, 2875–2880.
15 J. Barber, S. Morin and B. E. Conway, *J. Electroanal. Chem.*, 1998, **446**, 125–138.
16 J. Horiuti and T. Nakamura, *Adv. Catal.*, 1967, **17**, 1–73.
17 M. R. Gennero de Chialvo and A. C. Chialvo, *J. Electrochem. Soc.*, 2000, **147**, 1619–1622.
18 A. J. Bard and L. R. Faulkner, *Electrochemical Methods: Fundamentals and Applications*, J. Wiley & Sons, New York, 1980.
19 M. R. Gennero de Chialvo and A. C. Chialvo, *Electrochim. Acta*, 1998, **44**, 841–851.
20 D. Jahn and W. Vielstich, *J. Electrochem. Soc.*, 1962, **109** 849–852.